Available online at www.sciencedirect.com
ScienceDirect
Dyes and Pigments 76 (2008) 118–124
DYES and PIGMENTS
www.elsevier.com/locate/dyepig

Synthesis, structure and photophysical properties of three new hemicyanine dyes

Du-Xia Cao [a,*], Zhi-Qiang Liu [b], Guo-Hui Zhang [a], Feng-Xia Cao [a], Hong-Yu Chen [c], Guo-Zhong Li [a,*]

[a] School of Materials Science and Engineering, Jinan University, Jinan 250022, China
[b] State Key Laboratory of Crystal Materials, Shandong University, Jinan 250100, China
[c] Faculty of Chemistry and Chemical Engineering, Taishan Medical University, Taian 271016, China

Received 14 August 2006; accepted 17 August 2006
Available online 5 October 2006

Abstract

Three new hemicyanine dyes that feature a fixed pyridine cation as electron acceptor, *trans*,*trans*-4-{4-[4-(*N*,*N*-diphenylamino)styryl]styryl}-*N*-methylpyridinium iodide (**1**), *trans*,*trans*-4-{4-[4-(*N*-carbazolyl)styryl]styryl}-*N*-methylpyridinium iodide (**2**) and *trans*,*trans*-4-{4-[2-(benzothiazole-2-yl)ethenyl]styryl}-*N*-methylpyridinium iodide (**3**), have been synthesized. The crystal structure of dye **1** was determined. X-ray diffraction analyses reveal that **1** crystal belongs to monoclinic, $P2_1/c$ space group. Composite materials with these organic dyes doped into polymer-impregnated composite glass were prepared. Photophysical properties of these dyes in various solvents and composite glass were investigated in detail. Generally, photophysical properties of the dyes greatly increase in glass matrices compared with that in solution and there is no obvious fluorescence quenching in high doped concentration. The relationships between molecular structure and photophysical properties of this series of dyes were discussed.

Keywords: Hemicyanine dye; Composite glass; Crystal structure; X-ray diffraction; Photophysical properties

1. Introduction

Hemicyanine (aminostyryl pyridinium) dyes are a type of important functional dyes, which have been widely applied in many areas such as frequency-upconverted lasing [1], optical power limiting [2], fluorescence probes [3] and molecular electronics [4]. Especially, hemicyanine dyes attracted considerable research interests recently in two-photon pumped upconverted lasing due to their high upconverted efficiency and low threshold [5]. From the viewpoint of molecular engineering, structural features such as the π-conjugation style, the molecular planarity, and the length of conjugated bridge all play an important role in tuning nonlinear optical properties of materials [6]. A number of studies found that nonlinear optical effect increases with the increase of the length of conjugated bridge and molecular planarity [6,7]. Based on the ideas above, we synthesized three new hemicyanine dyes with two conjugated styryl units or diethenylphenyl as conjugated bridge and pyridine cation as electron acceptor.

However, a solution of organic dyes has limited application because of some disadvantages such as lack of chemical, thermal and photochemical stability, short lifetime and toxicity. So the optical active organic dyes are often introduced to a photostable medium such as polymer and/or glass matrix allowing their use as building blocks for photonic devices. SiO_2 sol–gel composite glass has perfect optical quality and can provide good luminescent environment for a lot of optical active materials [8]. Composite materials with organic dyes doping polymer-impregnated inorganic SiO_2 sol–gel composite glass will

* Corresponding authors. Tel.: +86 531 82765974; fax: +86 531 87974453.
E-mail addresses: duxiacao@ujn.edu.cn (D.-X. Cao), Ligz2201@163.com (G.-Z. Li).

0143-7208/$ - see front matter © 2006 Elsevier Ltd. All rights reserved.
doi:10.1016/j.dyepig.2006.08.013

integrate the advantages of organic molecules and inorganic glass, show potential applications in many fields [9,10]. In this work, we prepared composite materials with the synthesized organic dyes as dopant and SiO_2 sol–gel glass and poly methyl methacrylate (PMMA)/SiO_2 sol–gel composite glass as matrix. Photophysical properties of the dyes in various solvents and solid matrices were investigated in detail. The goal of the research presented herein is to investigate the structural and photophysical properties of new hemicyanine derivatives, which have potential for use in a number of different fields, such as two-photon upconverted lasing and optical power limiting.

2. Experimental section

2.1. Reagents and instruments

Nuclear magnetic resonance spectra were recorded on a MercuryPlus-400 spectrometer. Elemental analyses were carried out on a PE 2400 autoanalyzer. 2-Methylbenzothiazole and triphenylamine were obtained from Acros Ltd. 4-(*N*,*N*-Diphenylamino)benzaldehyde was prepared by a standard Vilsmeier reaction. 4-(*N*-Carbazolyl)benzaldehyde and 4-methyl-*N*-methylpyridinium iodide were synthesized according to procedures described in the literature [11]. Other reagents, such as *p*-phthaldehyde and piperidine were purchased from Shanghai Reagents and were used as received directly without further purification. All of the solvents were freshly distilled before use.

2.2. Synthesis and characterizations of dyes

The synthetic strategy for the preparation of the dyes is shown in Scheme 1. As outlined in Scheme 1, we synthesized the dyes by reduction, Wittig and subsequently concentration reaction. The detailed procedures are described below.

2.2.1. 4-[4-(N,N-Diphenylamino)styryl]aldehyde (1′)

4-(*N*,*N*-Diphenylamino)benzaldehyde was reduced by KBH_4 to 4-[(*N*,*N*-diphenylamino) benzyl] alcohol. The phosphonium salt **S-1** was prepared conveniently from 4-[(*N*,*N*-diphenylamino)benzyl] alcohol and 1 equiv $HBr^-P^+Ph_3$. Then **1′** was obtained by Wittig reactions using **S-1** and *p*-phthaldehyde.

S-1, 12 g (0.02 mol), 5.4 g (0.04 mol) *p*-phthaldehyde and 100 mL freshly distilled THF were added into 250 mL three-necked flask. Then 4.7 g (0.04 mol) potassium *tert*-butoxide in 100 mL THF was added dropwise under nitrogen with stirring in an ice-bath for 1 h. The mixture was continuously stirred at room temperature overnight. The mixture was poured into a beaker containing 200 mL distilled water. This mixture was extracted with chloroform, the organic phase was dried using anhydrous Na_2SO_4 and then the organic solvent was removed using a rotary evaporator. The crude product was recrystallized twice from ethanol to give yellow powders with a yield of 50%. M.p. 149–151 °C. ^{1}H NMR, δ ($CDCl_3$, 400 MHz): 6.93–7.39 (m, 16H), 7.54 (d, 2H, $J = 8.3$ Hz), 7.79 (d, 2H, $J = 8.3$ Hz), 9.90 (s, 1H).

2.2.2. 4-[4′-(N-Carbazolyl)styryl]aldehyde (2′)

Compound **2′** was prepared as yellow-green platelet crystals with a yield of 52% following a method similar to that used to prepare **1′**. M.p. 224–226 °C. ^{1}H NMR, δ ($CDCl_3$, 400 MHz): 7.21–7.76 (m, 14H), 7.84 (d, 2H, $J = 8.3$ Hz), 8.08 (d, 2H, $J = 8.3$ Hz), 9.95 (s, 1H).

2.2.3. 4-[2-(Benzothiazole-2-yl)ethenyl]aldehyde (3′)[12]

Compound **3′** was prepared by concentration reaction of 2-methylbenzothiazole and 1 equiv *p*-phthaldehyde. The crude product was recrystallized from ethanol to give yellow needle-like crystals with a yield of 80%. M.p. 159–160 °C. ^{1}H NMR, δ ($CDCl_3$, 400 MHz): 7.43 (t, 1H, $J = 7.6$ Hz), 7.51 (t, 1H, $J = 7.6$ Hz), 7.58 (d, 2H, $J = 3.4$ Hz), 7.76 (d, 2H, $J = 8.2$ Hz), 7.94 (d, 2H, $J = 8.2$ Hz), 7.91 (d, 1H, $J = 8.4$ Hz), 8.05 (d, 1H, $J = 8.1$ Hz), 10.05 (s, 1H).

2.2.4. trans,trans-4-{4-[4-(N,N-Diphenylamino)styryl]-styryl}-N-methylpyridinium iodide (1)

Compound **1′**, 0.3 g (0.0009 mol), 0.21 g (0.0009 mol) 4-methyl-*N*-methylpyridinium iodide (**S-3**), and 30 mL ethanol were added into a 100 mL one-necked flask with a stirrer and a condenser. Then three drops of piperidine were added. The solution was heated to reflux for 10 h. After the mixture had cooled to room temperature, a large amount of red precipitate formed. The separated precipitate was repeatedly washed with ethanol to give red microcrystals with a yield of 70%. M.p. 259–260 °C. ^{1}H NMR, δ (DMSO, 400 MHz): 3.36 (s, 3H), 6.92–7.17 (m, 9H), 7.29–7.33 (m, 5H), 7.48–7.52 (m, 3H), 7.71–7.73 (m, 4H), 7.98 (d, 1H, $J = 12.4$ Hz), 8.18 (s, 2H), 8.80 (s, 2H). Anal. calcd for $C_{34}H_{29}IN_2$ (592.52): C 68.92; H 4.93; N 4.73. Found: C 68.80; H 4.99; N 4.78.

2.2.5. trans,trans-4-{4-[4-(N-Carbazolyl)styryl]styryl}-N-methylpyridinium iodide (2)

By reaction of **2′** and **S-3**, **2** was prepared as a red powder with a yield of 65% following a method similar to that described above. M.p. 297–298 °C. ^{1}H NMR, δ (DMSO, 400 MHz): 3.34 (s, 3H), 7.29–7.43 (m, 7H), 7.49 (d, 2H, $J = 16$ Hz), 7.67 (d, 2H, $J = 8.4$ Hz), 7.79–7.80 (m, 7H), 8.20–8.29 (m, 4H), 8.83 (d, 2H, $J = 6.4$ Hz). Anal. calcd for $C_{34}H_{27}IN_2$ (590.51): C 69.16; H 4.61; N 4.74. Found: C 69.05; H 4.66; N 4.78.

2.2.6. trans,trans-4-{4-[2-(Benzothiazole-2-yl)ethenyl]-styryl}-N-methylpyridinium iodide (3)

By reaction of **3′** and **S-3**, **3** was prepared as yellow microcrystals with a yield of 75% following a method similar to that described above. M.p. 271–272 °C. ^{1}H NMR, δ (DMSO, 400 MHz): 3.32 (s, 3H), 7.44–7.56 (m, 2H), 7.61 (d, 1H, $J = 16.3$ Hz), 7.73 (d, 2H, $J = 3.8$ Hz), 7.83 (d, 2H, $J = 8.4$ Hz), 7.92 (d, 2H, $J = 8.4$ Hz), 7.99–8.05 (m, 2H), 8.12 (d, 1H, $J = 7.7$ Hz), 8.23 (d, 2H, $J = 6.7$ Hz), 8.88 (d, 2H, $J = 6.7$ Hz). Anal. calcd for $C_{23}H_{19}IN_2S$ (482.38): C

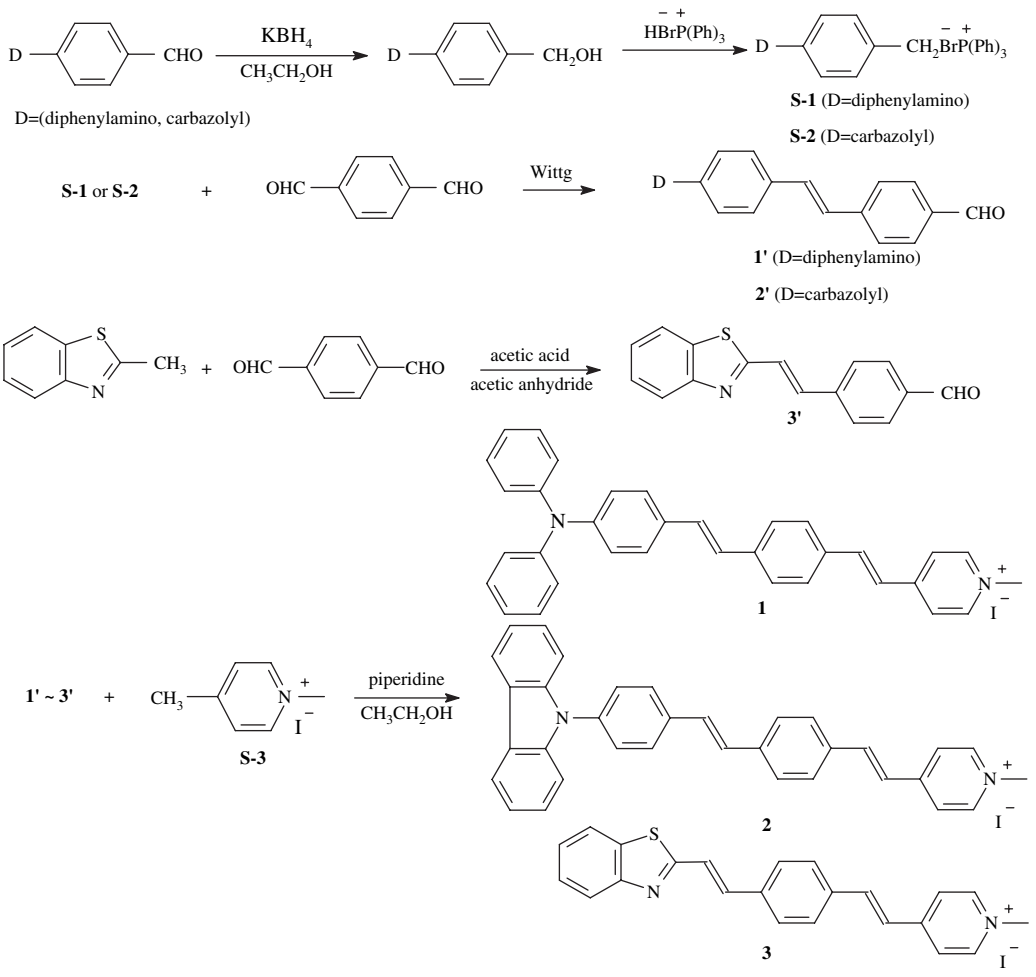

Scheme 1. Synthetic strategy for the preparation of the dyes.

57.27; H 3.97; N 5.81; S 6.65. Found: C 57.51; H 3.92; N 5.70; S 6.87.

2.3. Solution and solid state sample preparation

2.3.1. Solution sample preparation

Dye solutions with a series of concentrations were prepared in various solvents for absorption and emission measurements in order to study the effects of solvent and structure on the photophysical properties.

2.3.2. Solid state sample preparation

2.3.2.1. Preparation of composite materials with sol–gel glass as medium. At first, sol–gel glasses with pore volume of 70% were obtained according to Ref. [13]. The dyes were doped at the interfacial phase by placing the porous glass in acetonitrile solution of the dyes. After the solution completely impregnated the glass, the glass monolith was removed from the solution and placed in air for several hours until the solvent evaporated out of the glass. This procedure resulted in a solution of 70% acetonitrile concentration. This concentration is based on the volume of the pores of the glass being ~70% of the total volume, and it assumes that none of the chromophore evaporated/decomposed upon the removal of the solvent.

2.3.2.2. Preparation of composite materials with PMMA/SiO_2 sol–gel composite glass as medium. After the dyes were doped at the interfacial phase of the glass, the glasses were immersed in the MMA monomer solution with benzoyl peroxide (2%). Then the MMA solution diffused into the glass pores and was polymerized therein.

2.4. Structure determination

Single crystals of dye **1** suitable for X-ray structure determination were obtained by slow evaporation of acetonitrile solution of the dye. X-ray diffraction data of a red single crystal of **1** ($0.26 \times 0.13 \times 0.11$ mm) were collected on a Bruker Smartapex CCD diffractometer. The radiation sources were Mo Kα. Of 15 675 collected reflections ($4.18 \leq 2\theta \leq 50.02$), 5338 reflections were independent ($R_{int} = 0.0768$). By SHELXTL-97 program, the structure was resolved by direct method and refined by full-matrix least-squares method on F^2. The crystal belongs to the monoclinic, $P2_1/c$ space group, with a formula $C_{34}H_{29}IN_2 \cdot 2(H_2O)$ and molecular weight 626.51. $a = 8.3315(19)$, $b = 36.084(8)$, $c = 10.151(2)$ Å,

$\beta = 93.604(4)^\circ$, $V = 3045.6(12)$ Å^3, $Z = 4$, $D_c = 1.366$ Mg/m^3, $\mu = 1.083$ mm^{-1}, $F(000) = 1280$, $R_1 = 0.1292$, $wR_2 = 0.3867$ [$I > 2\sigma(I)$].

2.5. Photophysical properties' measurement

Linear absorption spectra of the dyes in various solvents and solid matrices were recorded on a Shimadzu UV2550 spectrophotometer. Steady-state fluorescence spectra were measured on an Edinburgh FLS920 fluorescence spectrometer equipped with a 450 W Xe lamp. All the solvents used for absorption and fluorescence measurements were HPLC grade.

3. Results and discussion

3.1. Structure features of *1*

There is one disorder that affects the C27 and C28 atoms in the π-bridge in the structure of **1**. The disorder is over two orientations and the disorder pairs have similar occupancy.

The molecular structure of **1** has been clearly characterized by several dihedral angles in the molecule. As shown in Fig. 1, the dihedral angle between the two phenyl rings (P1: C13 to C18, P2: C21 to C26) is 4.3(5)°, and the dihedral angle between P2 and pyride ring P3 (C29 to C33, N2) is only 1.5(5)°. These data indicate that the planarity of **1** is fairly good and the molecule is highly conjugated, which will be helpful to elucidate linear and nonlinear optical properties.

3.2. Linear photophysical properties in solution

The photophysical data of the dyes in various solvents and solid matrices are shown in Table 1.

3.2.1. The influence of molecule structure

Linear absorption and fluorescence spectra of dyes **1**–**3** in $CHCl_3$ are shown in Fig. 2. Dyes **1** and **2** possess similar molecular structure with different terminal electron donor group. In general, the structural factors, especially different end groups play an important role in determining the different photophysical properties of these dyes. Compared with **1**, absorption and fluorescence peaks of **2** are blue-shifted in every solvent, which may be derived from the weaker electron-donating ability of carbazolyl group in **2** than that of diphenylamino group in **1** [14]. Dye **2** processes larger absorbance and fluorescence intensity than **1** in any one solvent. The better photophysical properties of **2** may be derived from the more difficulty to twist because of larger rigidity of carbazolyl, and the charge-transferred excited emission state of **2** may comparatively be more stable against nonradiative decay. The molecule structure of dye **3** is very different from those of dyes **1** and **2**, which is an A–π–A′ type molecule with 2-benzothiazolyl and pyridine cation as electron acceptor group. Compared with **1** and **2**, absorption and fluorescence peaks of **3** are blue-shifted in every solvent because of less flowing π electron. But **3** possesses larger linear absorption and strong fluorescence, which may be derived from higher π conjugation. The benzothiazolyl acceptor is highly conjugated with the π-bridge and the whole molecule of the **3** possesses perfect planarity [14].

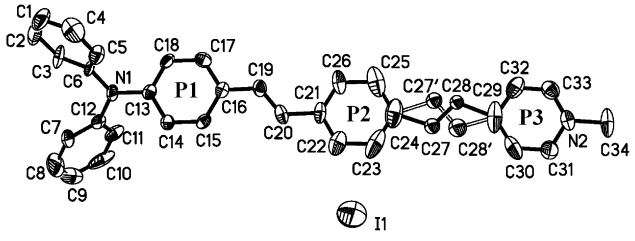

Fig. 1. The molecular structure of **1**.

3.2.2. The influence of solvent polarity

Based on Table 1, we can see that the linear absorption properties of all the dyes are strongly affected by the solvent polarity. From weak polarity solvent (toluene) to medium polarity solvent ($CHCl_3$), the absorption λ_{max} shows an obvious red shift and the absorbance increases sharply. But from $CHCl_3$ to strong polarity solvents (CH_3CN, DMF), the absorption λ_{max} shows a blue shift and the absorbance increases further.

The fluorescence properties of dyes **1** and **2** exhibit similar dependence on solvent polarity. A more quantitative scale for solvent polarity is based on the orientational polarizability (Δf) of the solvent. The orientational polarizability (Δf) is defined as [15]:

$$\Delta f = [(\varepsilon - 1)/(2\varepsilon + 1)] - \left[\left(n^2 - 1\right)/\left(2n^2 + 1\right)\right] \quad (1)$$

where ε and n are the dielectric constant and the refractive index of solvent, respectively. The value of Δf reflects the polarity of solvent. The properties of the solvents and glass matrices are shown in Table 2.

In $CHCl_3$ solution ($\Delta f = 0.1487$), **1** and **2** exhibit the strongest fluorescence emission and the longest fluorescence wavelength (shown in Fig. 3). Despite the dyes in strong polarity solvents (CH_3CN: $\Delta f = 0.2760$ and DMF: $\Delta f = 0.3062$) show the largest linear absorption, but the fluorescence of these is the weakest. The strong dependence of these photophysical properties on the polarity of the solvent may be explained by the twisted intramolecular charge transfer (TICT) model [16,17]. According to the TICT model, the molecules initially form a moderate polar fluorescence emission state. Subsequently, the molecules quickly undergo certain conformation isomerization of so-called twist, and this is accompanied by an intramolecular charge transfer from the donor to the acceptor. This TICT state is believed to be less emission and the polarity of the TICT molecule is supposed to be much larger than that of primarily excited state and its energy level is considerably lowered. With the increase of solvent polarity, the activation barrier for the TICT process decreases, this induces the decrease of fluorescence intensity. The weaker linear absorbance and fluorescence in toluene relative to that in $CHCl_3$ may be derived from less solubility. Toluene is a weak polar solvent with Δf being 0.0140 but the dyes are strong polar molecules. High polar molecules are not well "dissolved" in

Table 1
Photophysical properties of the dyes in various solvents and solid matrices

Dyes	Solvents	λ_{max}^{abs} (nm)	ε_{max} (10^4 cm^{-1} M^{-1})	λ_{max}^{fluo} (nm)	$\Delta\bar{\nu}$ (cm^{-1})
1	Toluene	310, 460	0.77, 0.54	642	6163
	$CHCl_3$	366, 489	1.64, 1.72	764	7361
	DMF	353, 444	1.34, 2.17	579	5251
	CH_3CN	352, 443	1.27, 2.19	574	5152
	Sol–gel glass	486		743	7117
	Composite glass	416		522	4881
2	Toluene	295, 376	1.27, 1.10	608	10 148
	$CHCl_3$	293, 429	0.85, 1.60	636	7587
	DMF	410	2.60	518	5085
	CH_3CN	408	2.66	520	5279
	Sol–gel glass	454		614	5740
	Composite glass	399		486	4487
3	Toluene	390	0.56	424	2056
	$CHCl_3$	406	3.49	516	5251
	DMF	393	4.35	542	6995
	CH_3CN	386	4.02	546	7592
	Sol–gel glass	400		535	6308
	Composite glass	382		529	7274

Linear absorption and fluorescence properties in solution and glass matrices were measured at $c = 1.0 \times 10^{-5}$ mol/L and $c = 1.0 \times 10^{-4}$ mol/L, respectively.

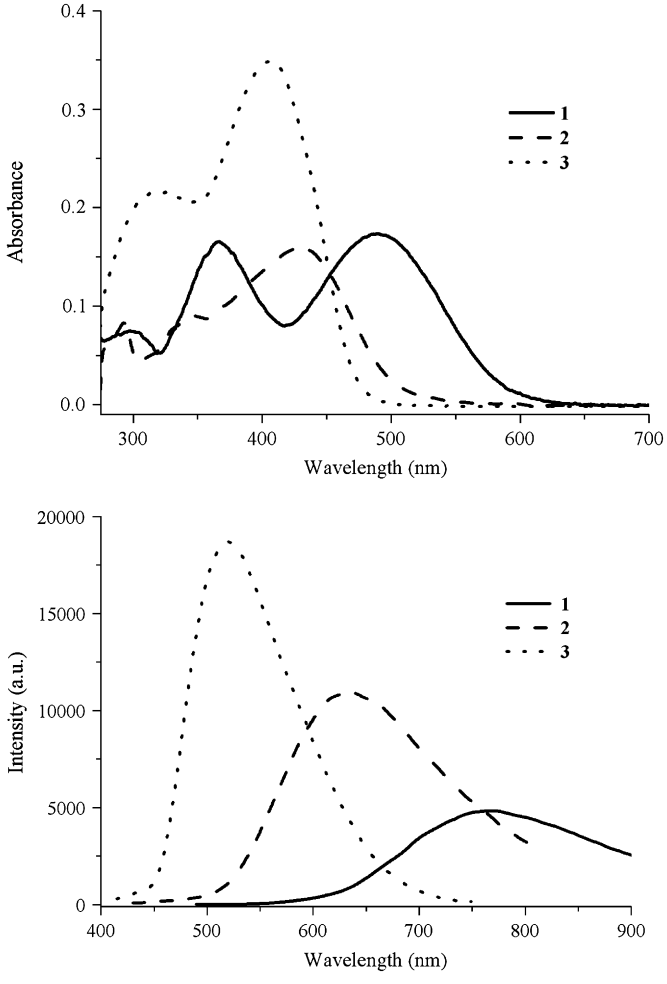

Fig. 2. Linear absorption (above) and fluorescence (below) spectra of **1**–**3** in $CHCl_3$ at $c = 1.0 \times 10^{-5}$ mol/L.

weak polar solvents but prefer to disperse into aggregates [18]. The weak absorption and fluorescence properties of toluene solution indicate that strong quenching occurred in the aggregates of model molecules. The strongest fluorescence intensity in chloroform solution is the result of integration of aggregation of molecules and TICT effect.

The structural properties of dye **3** are different from those of the other two dyes, so it exhibits different dependence on solvent polarity. As shown in Fig. 4, with the increase of the solvent polarity, the peak positions in the emission spectra of **3** are remarkably red-shifted and the intensity increases, which may be because of the fact that resolvability increases with solvent polarity.

3.3. Photophysical properties of the dyes in solid matrices

We also investigated the photophysical properties of the dyes in solid matrices (SiO_2 sol–gel glass, PMMA/sol–gel

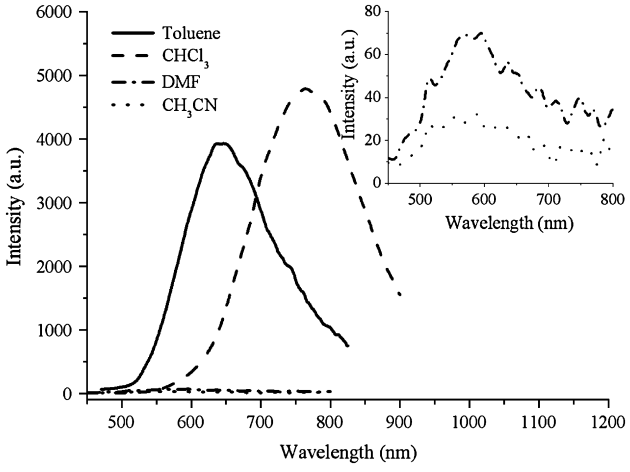

Fig. 3. Fluorescence spectra of dye **1** in various solvents at $c = 1.0 \times 10^{-5}$ mol/L.

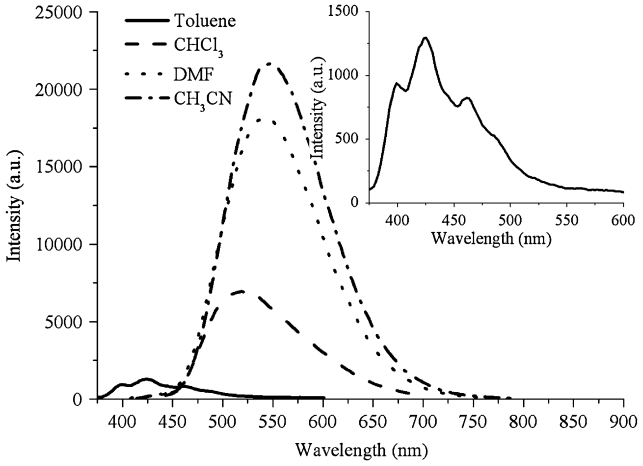

Fig. 4. Fluorescence spectra of dye **3** in various solvents at $c = 1.0 \times 10^{-5}$ mol/L.

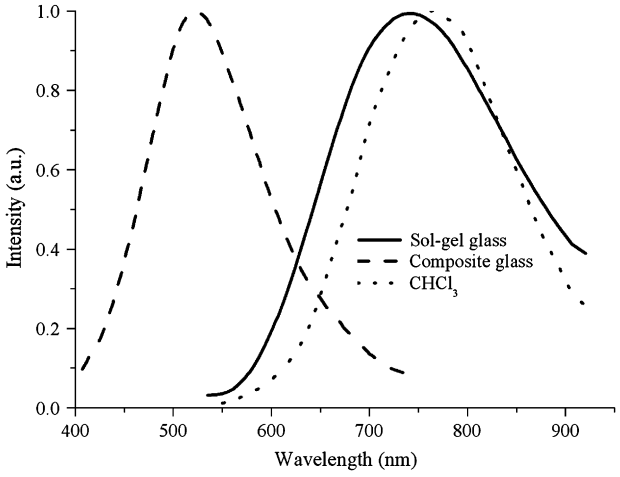

Fig. 5. Normalized fluorescence spectra of **1** in different microenvironments at $c = 1.0 \times 10^{-4}$ mol/L.

composite glass) considering application. The investigation indicates that the fluorescence intensity and stability of the dyes in solid matrices are higher than that in solution especially in PMMA/sol–gel composite glass. Fluorescence intensity in solid matrices basically builds up with the increase of the doped concentration. But fluorescence intensity in solution builds up with the increase of the concentration when the concentration is lower (lower than 5.0×10^{-5} mol/L), but fluorescence intensity decreases with the increase of the concentration when the concentration is higher, which indicates that strong fluorescence quenching occurred in concentrated solution because of the aggregates of molecules. In solid matrices especially composite glass, organic molecule is isolated by solid matrices, so the aggregate probability of molecules decreases greatly. We also found that the fluorescence intensity is weaker and color is deepened after organic molecule solution is placed in air for some time. But composite materials still retain primary properties.

Fig. 5 is normalized fluorescence spectra of dye **1** in a different microenvironment. The emission maximum of **1** in composite glass (522 nm) is blue-shifted compared to that in pure sol–gel glass (743 nm) and $CHCl_3$ solution (764 nm). The change in trend of **2** in different microenvironments is similar to that of **1**. But to **3**, emission maximum in composite glass (529 nm) is blue-shifted compared to that in pure sol–gel (535 nm) and red-shifted compared to that in $CHCl_3$ solution (516 nm). The fluorescence peak of **3** is red-shifted with the increase of microenvironment polarity in all matrices and the relationship between Stokes shifts ($\Delta\overline{\nu}$) and orientational polarizability (Δf) obeys the Lippert equation (shown in Fig. 6). Lippert equation describes the relationship between Stokes shift and orientational polarizability [15]:

$$\Delta\overline{\nu} = \overline{\nu}_a - \overline{\nu}_f = 2\Delta\mu_{ge}^2 \Delta f / hca^3 + \text{const} \quad (2)$$

In the above equation, $\Delta\overline{\nu} = \overline{\nu}_a - \overline{\nu}_f$ is the Stokes shift of the molecule, $\overline{\nu}_a$ and $\overline{\nu}_f$ are the wavenumbers of the absorption and emission maximum, respectively, h is Planck's constant, c is the speed of light, and a is the cavity radius of the molecule.

The experimental data of dyes **1** and **2** did not obey the Lippert equation, which may be because of some special reciprocity between organic molecule and microenvironment.

Table 2
Properties of solvents and glass matrices

	Toluene	$CHCl_3$	DMF	CH_3CN	Sol–gel glass	Composite glass
n	1.494[a]	1.444[a]	1.427[a]	1.342[a]	1.444[b]	1.474[b]
ε	2.379[a]	4.806[a]	37.6[a]	37.4[a]	55[b]	7.8[b]
Δf	0.0140	0.1487	0.2760	0.3062	0.277	0.191

[a] The values of solvents are taken from Ref. [19].
[b] Data are taken from Ref. [20].

4. Conclusions

We have synthesized three new hemicyanine dyes and investigated their photophysical properties in different microenvironments. The photophysical data indicate that doping dyes

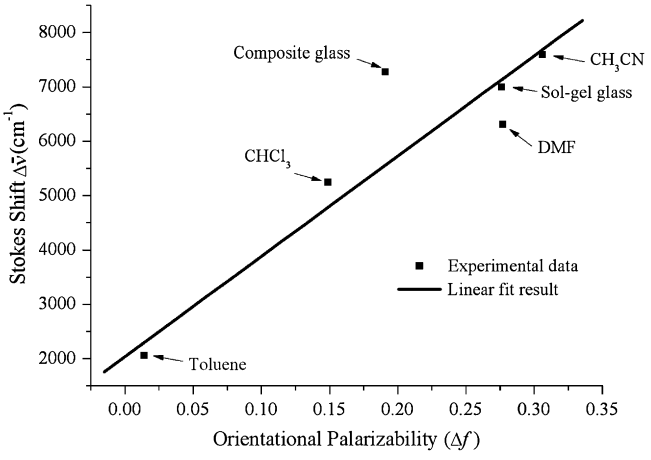

Fig. 6. Lippert plot (Stokes shift $\Delta\overline{\nu}$ vs orientational polarizability Δf for **3**. (The scatter dots are the experimental data and the line is the linearly fitted result.)

in a composite glass prevent the formation of aggregates and then the photophysical properties and stability increase in composite glass relative to solution. So composite glass is a good candidate as host matrices for organic dyes in advanced optics applications.

5. Supplementary material

Crystallographic data for the structure reported in this paper have been deposited with the Cambridge Crystallographic Data Centre as supplementary publication no. CCDC 616601. Copies of the data can be obtained free of charge on application to CCDC, 12 Union Road, Cambridge CB2 1EZ, UK (fax: 44 1223 336 033; e-mail: deposit@ccdc.cam.ac.uk).

Acknowledgments

This work was supported by the Doctoral Fund of Jinan University (no. B0415).

References

[1] Zhao CF, Gvishi R, Narang U, Ruland G, Prasad PN. J Phys Chem 1996;100:4526–32.
[2] He GS, Bhawalkar JD, Zhao CF, Prasad PN. Appl Phys Lett 1995;67:2433–5.
[3] Jędrzejewska B, Kabatc J, Pietrzak M, Pączkowski J. Dyes Pigments 2003;58:47–58.
[4] Huang YY, Cheng TR, Li FY, Luo CP, Huang CH, Cai ZG, et al. J Phys Chem B 2002;106:10031–40.
[5] Wang XM, Zhou YF, Yu WT, Wang C, Fang Q, Jiang MH, et al. J Mater Chem 2000;10:2698–703.
[6] Albota M, Beljonne D, Brédas JL, Ehrlich JE, Fu JY, Heikal AA, et al. Science 1998;281:1653–6.
[7] Ventelon L, Charier S, Moreaux L, Mertz J, Blanchard-Desce M. Angew Chem Int Ed 2001;40:2098–101.
[8] Gvishi R, Narang U, Ruland G, Kumar DN, Prasad PN. Appl Organomet Chem 1997;11:107–27.
[9] Li X, King TA, Pallikari-Viras F. J Non-Cryst Solids 1994;170:243–9.
[10] Pérez-Bueno JJ, Díaz-Flores LL, Pérez-Robles JF, Espinpoza-Beltrán FJ, Ramírez-Bon R, Vorobiev YV, et al. Microelectro Eng 2000;51–52:667–75.
[11] Zhao CF, He GS, Bhawalkar JD, Park CK, Prasad PN. Chem Mater 1995;7:1979–83.
[12] Huang ZL, Lei H, Li N, Qiu ZR, Wang HZ, Guo JD, et al. J Mater Chem 2003;13:708–11.
[13] Gvishi R, He GS, Prasad PN, Narang U, Li M, Bright FV, et al. Appl Spectrosc 1995;49:834–9.
[14] Cao DX, Fang Q, Wang D, Liu ZQ, Xue G, Xu GB, et al. Eur J Org Chem 2003;3628–36.
[15] Lakowicz JR. Principles of fluorescence spectroscopy. New York: Plenum Press; 1983. p. 190.
[16] Sarkar N, Das K, Nath DN, Bhattacharyya K. Langmuir 1994;10:326–9.
[17] Grabowski ZR, Dobkowski J. Pure Appl Chem 1983;55:245–52.
[18] Tian ZY, Chen Y, Yang WS, Yao JN, Zhu LY, Shuai ZG. Angew Chem Int Ed 2004;43:4060–3.
[19] Ren Y, Yu XQ, Zhang DJ, Wang D, Zhang ML, Xu GB, et al. J Mater Chem 2002;12:3431–7.
[20] Gvishi R, Narang U, Bright FV, Prasad PN. Chem Mater 1995;7:1703–8.